Climatic Change (2014) 122:283–298
DOI 10.1007/s10584-013-1012-0

Impact of anthropogenic CO_2 on the next glacial cycle

Carmen Herrero · Antonio García-Olivares · Josep L. Pelegrí

Received: 5 February 2013 / Accepted: 19 November 2013 / Published online: 6 December 2013

Abstract The model of Paillard and Parrenin (Earth Planet Sci Lett 227(3–4):263–271, 2004) has been recently optimized for the last eight glacial cycles, leading to two different relaxation models with model-data correlations between 0.8 and 0.9 (García-Olivares and Herrero (Clim Dyn 1–25, 2012b)). These two models are here used to predict the effect of an anthropogenic CO_2 pulse on the evolution of atmospheric CO_2, global ice volume and Antarctic ice cover during the next 300 kyr. The initial atmospheric CO_2 condition is obtained after a critical data analysis that sets 1300 Gt as the most realistic carbon Ultimate Recoverable Resources (URR), with the help of a global compartmental model to determine the carbon transfer function to the atmosphere. The next 20 kyr will have an abnormally high greenhouse effect which, according to the CO_2 values, will lengthen the present interglacial by some 25 to 33 kyr. This is because the perturbation of the current interglacial will lead to a delay in the future advance of the ice sheet on the Antarctic shelf, causing that the relative maximum of boreal insolation found 65 kyr after present (AP) will not affect the developing glaciation. Instead, it will be the following insolation peak, about 110 kyr AP, which will find an appropriate climatic state to trigger the next deglaciation.

Keywords Climate change · Paleoclimate · Relaxation models · Glacial oscillations · Anthropogenic perturbation · Future earth climate

A. García-Olivares (✉) · C. Herrero
Institut de Ciències del Mar, CSIC,
Passeig Marítim de la Barceloneta 37-49, 08003 Barcelona, Spain
e-mail: agolivares@icm.csic.es

C. Herrero
e-mail: herrero@icm.csic.es

J. L. Pelegrí
LINCGlobal, Institut de Ciències del Mar, CSIC,
Passeig Marítim de la Barceloneta 37-49, 08003 Barcelona, Spain
e-mail: pelegri@icm.csic.es

1 Introduction

The control of the Pleistocene glacial-interglacial oscillations by orbital parameters (Milankovitch theory) is nowadays largely accepted (e.g., Hays et al. 1976; Paillard 2010). During the late Pleistocene, specifically the last 800 kyr, the climate has shown a remarkable 100-kyr ice-age cycle, recorded in Antarctic ice and deep-ocean sediment core records (Petit et al. 1999; Indermuhle et al. 2000; Monnin et al. 2001; Siegenthaler et al. 2005; Luthi et al. 2008; Lisiecki and Raymo 2005). This alternation between glacial and interglacial states has been attributed to a complex set of processes that involve orbital forcing and internal interactions and feedbacks in the climate system, yet to be properly precised (Archer et al. 2000; Sigman and Boyle 2000).

Following Paillard and Parrenin (2004), several relaxation models, based on simple parameterizations of deep ocean stratification, have been recently developed (García-Olivares 2012a, b). Two of these models, hereafter 3τ and LS, have good skills reproducing the conditions during the last 8 glacial cycles. The 100 kyr glacial-interglacial periodicity is internally generated through three coupled variables: atmospheric CO_2 concentration, global ice volume and the extension of the Antarctic ice shelf; an important mechanism is the advance and retreat of Antarctic ice as it controls, through brine formation, the deep-ocean stratification and, thus, its capacity to retain CO_2.

This paper will use these two models to predict the Earth's glacial-interglacial response during the forthcoming 300 kyr. In Section 2 the fundamental equations are presented and the models' good performance on reproducing past climates is illustrated. In Section 3, taking into account the history and predictions of anthropogenic CO_2 emissions, the fraction that remains in the atmosphere is specified. In Section 4 the models are applied to project the future climate with and without this anthropogenic CO_2 pulse. A discussion of our results, comparing them with those from other models, is presented in Section 5. We close with some brief conclusions in Section 6.

2 The 3τ and LS models

The 3τ and LS models (García-Olivares and Herrero 2012b) predict the time evolution of three dimensionless variables: V, representing global ice volume, forced by the atmospheric CO_2 and northern Hemisphere summer insolation (I_{65}, as calculated by Berger (1978) where time zero corresponds to 1950); atmospheric CO_2 concentration, C, linked to global ice volume and deep-ocean inorganic carbon contribution, which depends as a Heaviside step function ($H = 1$ if $F < 0$; $H = 0$ otherwise) on ocean stratification, F; and the extent of Antarctic ice sheet, A, which is forced by sea level changes through V (model 3τ) or by Antarctic temperature through C (model LS). The model equations are:

$$\begin{array}{cc} 3\tau & LS \\ \dfrac{dV}{dt} = \dfrac{(V_r - V)}{\tau_V} & \dfrac{dV}{dt} = \dfrac{(V_r - V)}{\tau_V} \end{array} \quad (1)$$

$$\dfrac{dA}{dt} = \dfrac{(V - A)}{\tau_A} \qquad \dfrac{dA}{dt} = \dfrac{(-C - A)}{\tau_A} \quad (2a;\ 2b)$$

$$\dfrac{dC}{dt} = \dfrac{(C_r - C)}{\tau_C} \qquad \dfrac{dC}{dt} = \dfrac{(C_r - C)}{\tau_C} \quad (3)$$

$$V_r = -xC - yI_{65} + z \qquad V_r = -xC - yI_{65} + z \tag{4}$$

$$C_r = -\beta V + \gamma H(-F) + \delta \qquad C_r = \alpha I_{65} - \beta V + \gamma H(-F) + \delta \tag{5a; 5b}$$

$$F = aV - bA + d \qquad F = -cC - bA + d \tag{6a; 6b}$$

In these equations the principal dependent variables V, A and C, tend exponentially to reference states V_r, A_r and C_r with characteristic times τ_V, τ_A and τ_C, respectively; these characteristic times change from one model to another (Table 1).

There are several differences between models 3τ and LS. One difference is the value used for the reference Antarctic ice sheet, either $-C$ (representing the inverse effect of Antarctic temperature on Antarctic ice sheet extent) for model LS or V for model 3τ. Another minor difference is the inclusion of I_{65} in model LS when specifying the reference atmospheric CO_2 concentration value, C_r. However, the main difference between both models is their parameterization of stratification, with $F = F(V, A)$ in model 3τ and $F = F(C, A)$ in model LS. Both V and C are good proxies for the Southern Ocean (SO) regional temperature and either $F = F(V, A)$ or $F = F(C, A)$ are plausibly ways to model the local formation of brines. The fact that the dependence $F = F(V, A)$ performs somewhat better than $F = F(C, A)$ may be due to the non-negligible role that V has on stratification through teleconnections (García-Olivares and Herrero 2012b) or to a possible larger effect of sea level than Antarctic temperature on brine formation.

Table 1 Parameter values used in 3τ and LS models

Parameter	3τ	LS model
τ_V	16585	11325
τ_{V2}	3105.5	2325
τ_C	13505	2793
τ_{C2}	–	8414
τ_A	9004	10266
x	0.905	0.669
y	0.489	0.527
z	0.946	0.761
α	–	0.237
β	0.336	0.793
γ	2.044	1.955
δ	0.228	0.146
a	0.54	–
b	1.205	0.936
c	–	0.533
d	0.483	0.069
R_V	0.88 /0.90	0.87 / 0.89
R_C	0.79	0.76

R_V and R_C represent the correlation between proxy and modelled data for global ice volume, V, and atmospheric CO_2 concentration, C, respectively. The two values displayed for R_V correspond to the correlations with the $\delta^{18}O$ and ice volume (Bintanja et al. 2005) time series, respectively

The calibration of model LS was done using a genetic algorithm for $\delta^{18}O$ and CO_2 data (Lisiecki and Raymo 2005; Petit et al. 1999; Indermuhle et al. 2000; Monnin et al. 2001; Siegenthaler et al. 2005; Luthi et al. 2008) in the interval (−600 kyr, −200 kyr); hereafter we will use negative and positive values when respectively referring to times before present (BP) and after present (AP), where year zero is taken as 1950 AD. The best-fit parameters were then used to validate the whole interval (−800 kyr, 0) with equally good performance. Model 3τ was calibrated directly for the whole interval (−800 kyr, 0), again using a genetic algorithm for the same two data sets.

The best-fit correlations were 0.87/0.88 (between $\delta^{18}O$ and modelled V) and 0.76/0.79 (between the reconstructed atmospheric CO_2 concentration and modelled C) for models LS/3τ. The results are not much sensitive to some smoothing in the time series; for example, if we use the best-fit model 3τ parameters, the correlation with the $\delta^{18}O$ series increases from 0.879, when using the raw data, to 0.882, after smoothing with a 2 kyr moving average.

The best-fit ice volume time series was then validated with the Bintanja et al. (2005) ice volume time series, which aims at removing the temperature effect from the $\delta^{18}O$ time series. The correlation improved further to 0.89 and 0.90 for models LS and 3τ, respectively, suggesting that our calibration with those uncorrected data has indeed produced a robust result. The parameter values that lead to the best data fit for either model are shown in Table 1.

The models, when using the parameters in Table 1, are able to reproduce the climatic maxima and minima observed from 800 kyr BP to the present for both ice volume and CO_2 (Fig. 1), as well as some of the observed suborbital periodicities. Cross-wavelet coherence

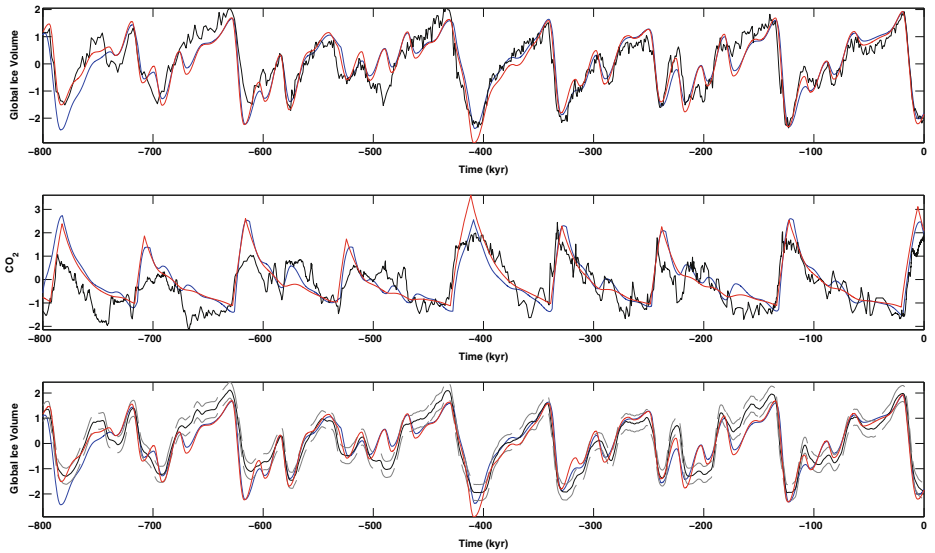

Fig. 1 *Top panel*: normalized ice volume as predicted with the LS (*blue line*) and 3τ (*red line*) models and proxy $\delta^{18}O$ records from Lisiecki and Raymo (2005) (*black line*). *Intermediate panel*: normalized CO_2 as predicted with the LS (*blue line*) and 3τ (*red line*) models and proxy data (Petit et al. 1999; Indermuhle et al. 2000; Monnin et al. 2001; Siegenthaler et al. 2005; Luthi et al. 2008) (*black line*). *Bottom panel*: Comparison of the normalized ice volume as predicted by the 3τ and LS models (red and light blue lines, respectively) with the relative sea level as obtained by Bintanja et al. (2005) (*black line*). The ±10 m error margins for the sea level data (approximately equivalent to one-sigma error in most of the series) are shown as *gray lines*

and cross-recurrence analyses (Grinsted et al. 2004; Marwan and Kurths 2002; Marwan et al. 2007) using proxy and simulated time series show that both model and proxy records display similar dynamics (García-Olivares and Herrero 2012b).

These results strongly endorse the idea that the relaxation models, despite their simplicity, do include some of the key mechanisms that are behind Pleistocene climatic oscillations. In fact, the models structure mimic some of the major feedbacks that are plausibly taking place in the mechanisms controlling the climate system, such as the effect of northern insolation at the solstice on ice volume, the CO_2 – temperature feedback (through ice volume V), the ice volume – CO_2 sources feedback, and the emission of deep-ocean CO_2 as a function of stratification (the variable F) in both models, which depends on sea level (SO temperature, represented by C in LS model) and Antarctic ice sheet extent. Additional details on these mechanisms, and the way the models represent them, can be found in Paillard and Parrenin (2004), Paillard (2010) and García-Olivares and Herrero (2012b).

Under these considerations, and provided the anthropogenic CO_2 pulse is properly represented, the models may be used to predict its effect on the perturbation of the natural sequence of glaciations and terminations.

3 Anthropogenic CO_2 emissions

3.1 Total CO_2 emission

A crucial first step is to estimate how much anthropogenic CO_2 will be emitted to the atmosphere. With this objective we use the historical record of burning fossil fuels (Boden et al. 2010), complemented with data for the last years obtained from the Global Carbon Project (http://www.globalcarbonproject.org/carbonbudget/). The annual rate of fossil fuels emission, E in (Gt yr^{-1}), is approximated through the following Lorentz function:

$$E = \frac{Ube^{-b(t-t_p)}}{\left[1+e^{-b(t-t_p)}\right]^2} \tag{7}$$

where U represents the Ultimate Recoverable Resources (URR) of fossil fuels in gigatons of carbon equivalent (Gtce), t_p is the year of peak fossil fuels emission (yr), and $Ub/4$ is the corresponding peak rate of fossil fuels emission (Gtce yr^{-1}). Only two of the three parameters are independent, e.g., given either the total area under the curve (U) or the year for peak emissions (t_p) we select the other two parameters by numerically searching the best least square fit of the data to Eq. 7.

The Intergovernmental Panel on Climate Change (IPCC) published a Special Report on Emission Scenarios (SRES) that contains 40 scenarios for future fossil fuel production to assess future climate change (SRES 2000). For example, the SRES A1 set uses an average accumulated carbon emission between 1750 and 2100 AD of approximately 1995 Gtce, and the A1F1 extreme scenario implicitly assumes 4100 Gtce of URR, according to the Hubbert linearization done by Berg and Boland (2013). However, these scenarios are based on simple extrapolations of present emission rates with no consideration on actual URR values. Höök et al. (2010) and Berg and Boland (2013) show that this report is based on unreasonably optimistic expectations about future fossil fuel production which do not take into account realistic estimates for proven and probable fossil fuels reserves. In order to obtain a realistic

estimate for U we have used the analysis of both Laherrere (2006) and the Energy Watch Group (2007) on the URR for the three main fossil fuels (coal, oil and gas).

The Energy Watch Group (2007) estimates 479 Gt for bituminous coal and anthracite, 272 Gt for sub-bituminous coal, and 158 Gt for lignite. Assuming 92 %, 40 % and 66 % of carbon respectively for these three minerals, we obtain approximately 558 Gtce and the peak of coal-derived CO_2 emissions on year 2042 AD. The analysis of Laherrere (2006) gives an estimate of 3000 Gb for all kind of oils (Gb = Gigabarrel, one oil barrel is very close to 159 liters of oil), which amounts to 353 Gtce if we use the conversion factor recommended by the US Environmental Protection Agency (http://www.epa.gov/greenpower/pubs/calcmeth.htm): 0.118 tons of carbon per barrel. The International Energy Agency (IEA 2010, 2012) recognizes that conventional oil production is at or very close to a maximum since 2006 AD and that this production will hardly increase much more, which amounts to an implicit recognition of the oil peak arrival (Laherrere 2012a). Regarding gas, Laherrere (2006) predicts an URR of 9100 Tcf, which amounts to about 120-132 Gt of carbon. Recently, Laherrere (2012b) has updated the URR coal estimate to 750 gigatons of oil equivalent (Gtoe). Using a carbon content of 25.7 tce/TJ for average coal, in the upper range of reported values (Gassan-zade 2004), this amounts to 808 Gtce. Given these considerations, the total fossil fuels URR amounts to approximately 1300 Gtce, being this our best estimate for the integrated anthropogenic emission of carbon.

Figure 2 shows the historical data on fossil fuels emissions during the 1800 to 2010 AD period and the corresponding fit using a Lorentz function (7), obtained setting $U = 1300$ Gt, which corresponds to a peak emissions on year 2037 AD. This fit has been done such that the integrated carbon emission at 2010 AD has exactly the same area than the historical time-series until 2010 AD (dashed lines in Figs. 2 and 3). This modified Lorentz function is the one we use to produce the full time series for the accumulated anthropogenic emission of fossil fuels (Fig. 3). The peak of emissions occurs in year 2037 AD, coincident with the inflexion point in the accumulated curve, and tends to zero near year 2324 AD, when the accumulated emissions reach their maximum values.

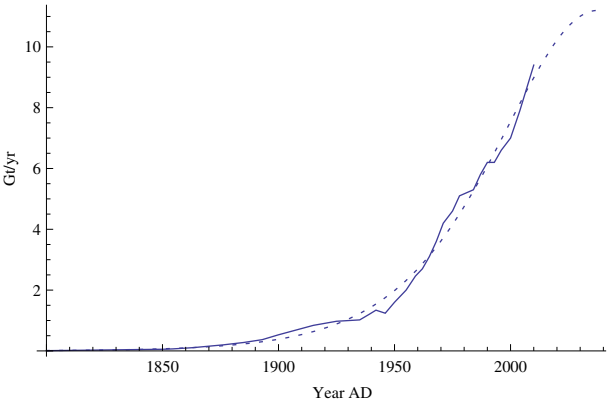

Fig. 2 Historical data of fossil fuels emissions during the 1800–2010 period (*continuous line*) and slightly modified Lorentz function such that the area until 2010 equals the accumulated historical emissions (*dashed line*)

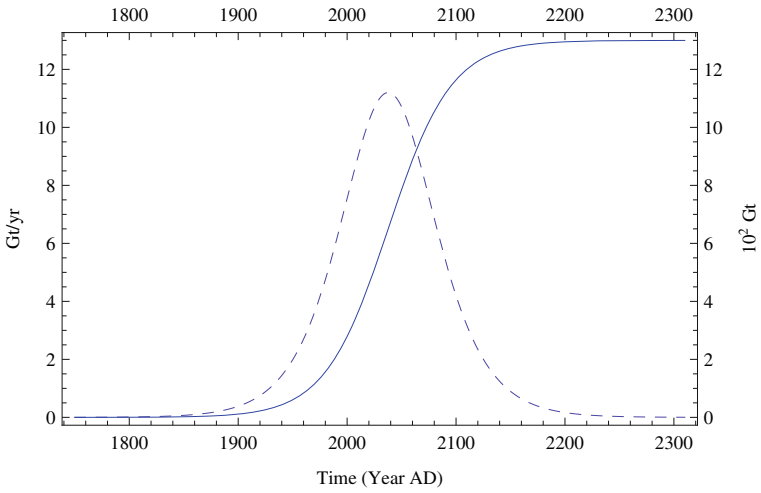

Fig. 3 Modified Lorentz function illustrating the anthropogenic carbon release per year (*dashed line*) and the accumulated carbon release (*solid line*)

3.2 CO_2 atmospheric response

The relatively fast, at the 10 to 100 yr scale, anthropogenic CO_2 emission will lead to a rise in atmospheric concentration but it will also produce an increased storage rate into the ocean, ground vegetation, trees, detritus and soil (Kheshgi and Jain 2003). Our models do not include this type of relatively rapid feedback climatic mechanisms. To take them into account we require a transfer function of accumulated carbon emissions (Ac, in Gt) to atmospheric CO_2 concentration (pCO_2, in ppmv). With this objective we turn to the global compartmental model ISAM (Jain et al. 1994; Kheshgi and Jain 2003), which may be interactively run online (http://climate.atmos.uiuc.edu/isam2/). In this model, the rates of transfer from the atmosphere to the above five compartments have been calibrated to match the average projections (by six dynamic global-vegetation models and 10 coupled ocean-atmosphere models) for CO_2 uptake between years 2000 and 2200 AD.

In order to obtain the Ac to pCO_2 transfer function, we use the ISAM model with the A1T scenario parameters, as proposed by the IPCC (SRES 2000). We run the ISAM model for values of URR between 0 and 3000 Gt, at increasing URR intervals of 100 Gt or better, replacing the fossil fuels input of A1T scenario with the modified Lorentz function. For each URR value we obtain the corresponding atmospheric response; these final response points are then linearly interpolated in order to have a continuous curve (Fig. 4). The corresponding transfer function should be adequate to model the short-term (at decadal and century time scales) response in the range from 0 to 3000 Gt; in particular, it may be used to model the results with our URR best estimate, $U = 1300$ Gt (Figs. 2 and 3). Note that contributions from future deforestation are considered by the ISAM model, therefore they are reflected in the transfer function of Fig. 4.

We may now finally estimate the time evolution of the anthropogenic atmospheric CO_2 pulse. The historical data of atmospheric concentrations is used for the period between 1750 and 2010 AD. Thereafter, and until the end of the anthropogenic emission in year 2324 AD, the atmospheric CO_2 is estimated using the predicted accumulated emissions from the modified Lorentz function (Figs. 2 and 3) and the transfer function as deduced from the

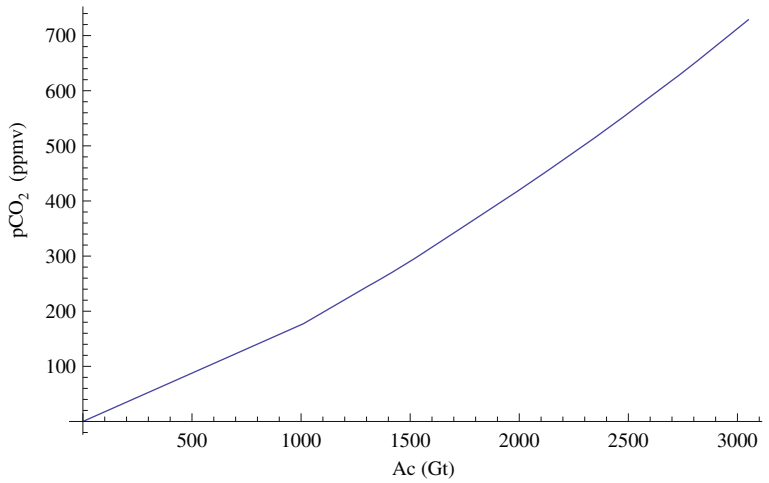

Fig. 4 Relation between the accumulated anthropogenic carbon emissions (Ac) and the atmospheric CO_2 concentration (pCO_2). The data is obtained from an aggregate of A1T scenarios (SRES 2000) as predicted by model ISAM (Jain et al. 1994), available at http://climate.atmos.uiuc.edu/isam2/, for every possible value of URR

ISAM model (Fig. 4). In this way the accumulated carbon emission is 361 Gt in year 2010 AD, 642 Gt in year 2037 AD, and reaches a maximum value of 1300 Gt by year 2324 AD, and the atmospheric concentrations at those dates can be obtained from the corresponding ordinates in Fig. 4.

4 Projections for the next glacial cycle

Before making a projection for the next 300 kyr we must take into consideration if there are other plausible mechanisms which are not incorporated in our models. In this work we consider two potential contributions: the very well established weathering compensation mechanism and the less known emission of methane from clathrates. We have chosen these two mechanisms not only because they are indeed relevant effects but also because they are illustrative of the sort of modifications that feedback mechanisms may cause in the Pleistocene dynamics.

According to Archer and Ganopolski (2005), the silicate weathering cycle will cause that 7 % of the anthropogenic CO_2 will still remain in the atmosphere 100 kyr after an anthropogenic perturbation. This implies that, after ending the anthropogenic emission, about 9 % of the CO_2 concentration will decay with a time constant of approximately 400 kyr. We take into consideration this non-linear buffer (ocean carbon chemistry) effect by simply assuming that 91 % of the anthropogenic perturbation will follow the dynamics given by Eqs. 1 to 6a, 6b while the remaining 9 % will have a long-term decay, with a 400 kyr time decay constant. A similar approach was used by Paillard (2006).

Archer et al. (2009) have studied the greenhouse effect expected to occur in the next 10 kyr as the rising temperatures lead to the emission of a fraction of the methane clathrates from continents and shelves. Their projection has a large uncertainty related to determining the critical fraction of methane bubbles that are able to reach the ocean surface. Taking this

fraction as 2.5 % and considering a scenario of 1000 Pg of carbon emission, sufficiently close to the one used in our models, he predicts an increase of 0.4–0.5 °C related to the escape of methane during some 10 kyr. Taking a climate sensitivity of 3 °C for a doubling of CO_2, the effect of the predicted methane emission, C_{met}, is equivalent to 40.5 ppmv of CO_2 concentration during a period of about 10 kyr. We have introduced this contribution in our projections by assuming that C_{met} (additional equivalent CO_2 concentration derived from methane) grows linearly from 0 to 40.5 ppmv between 0 and 2 kyr, remains constant between 2 and 10 kyr, and decreases linearly from 40.5 ppmv to 0 between 10 and 20 kyr.

Following these considerations, we are now ready to start the projection. The model Eqs. 1–6a, 6b are integrated forward, with the anthropogenic carbon emission scenario in Fig. 3 as the initial condition and properly forced by the insolation at 65 °N (Berger 1978), to predict the evolution of the interglacial-glacial transitions during the next 300 kyr. In order to obtain a CO_2 projection in dimensional units (ppmv), rather than the model non-dimensional units (Fig. 1), a concentration of 280 ppmv is assumed for year 1750 AD and a dimensional scale is obtained by considering the range of atmospheric concentrations in the Taylor Dome Ice Core between the last glacial maximum (181 ppmv) and year 1750 AD (280 ppmv) (Indermuhle et al. 2000). Similarly, in order to transform from model ice volume to benthic $\delta^{18}O$, the following conversion is used: $V = V_{nor} std(\delta^{18}O) + mean(\delta^{18}O)$, where V_{nor} is the modelled ice volume normalized with its own standard deviation and mean. All other variables remains non-dimensional as there is no dimensional scale available for their transformation.

The projection for the next 300 kyr is computed for both unperturbed and perturbed conditions using either the 3τ or LS models; Fig. 5 illustrates, as an example, the predicted evolution of atmospheric CO_2 following the anthropogenic CO_2 pulse. Both models display an exponential decay in atmospheric CO_2, with characteristic time decay somewhat longer for 3τ than for LS. The two models, despite having different parameterizations for ocean stratification and ice sheet evolution, do produce a very similar outcome for the following glacial cycle. Hereafter, we will focus on the future projection obtained with the 3τ model, a comparison of both models shows analogous results.

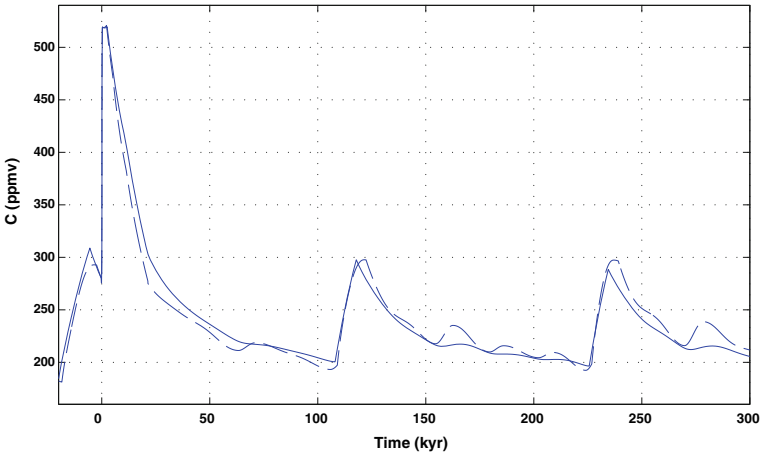

Fig. 5 Prediction of the dimensional atmospheric CO_2 concentration for the next 300 kyr using, as an initial condition, the anthropogenic carbon release scenario shown in Fig. 3. The continuous and dashed lines correspond to the projection with the 3τ and LS models, respectively

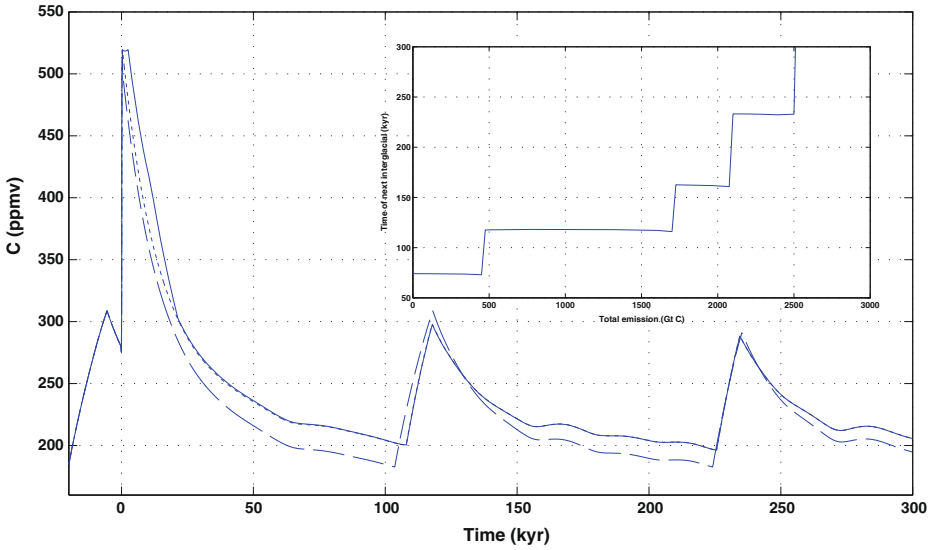

Fig. 6 Dimensional atmospheric CO_2 concentration for the next 300 kyr as predicted by model 3τ following the anthropogenic short-term pulse (*dashed line*), after adding the long-term weathering compensation (*dotted line*), and after further incorporating the methane emissions from clathrates (*continuous line*). The inset shows how the start of the next interglacial shifts depending on the total emissions of carbon

Figure 6 shows the CO_2 evolution predicted by model 3τ (Section 2) following the anthropogenic short-term pulse (Section 3.2), as well as including both long-term weathering and methane emissions. It may be observed that in all cases the timing for the next interglacials does not substantially change. The main effect is caused by the weathering compensation which causes somewhat higher concentrations and a slightly longer duration of the present interglacial. The effect of the methane emission is much reduced except for a a relatively short plateau in CO_2 values after ending the anthropogenic pulse.

The introduction of the anthropogenic CO_2 pulse clearly perturbs the natural cycle for all four model variables during the forthcoming 300 kyr (Fig. 7). Notice that the values for variables I_{65}, V, A and F in Fig. 7 are relative variations, only C has been translated to physical units (ppmv); further note that a minimum bound for V has been set to an additional 10 meters sea level rise with respect to year zero, which corresponds to a melting about 30 % higher than the Greenland ice sheet (IPCC 2001) and, for this reason, V doesn't take values under $-0.93/-1.94$ for 3τ /LS models.

A comparison between the different panels in Fig. 7 illustrates the influence of I_{65} on the sequence of events, as discussed in detail by García-Olivares and Herrero (2012b). In both the perturbed and unperturbed simulations, a V minimum (maximum) is produced a few thousand years after every positive (negative) peak in I_{65}. During a glaciation, the long-term increase in V produces an increase in A which tends to decrease the F value (due to the inverse dependence of F on A, Eq. 6a). The transit to the interglacial relies heavily on F turning negative (through the Heaviside function in Eq. 5a): F reaches negative values only during periods of advanced glaciation because at those times A is also large. In these situations, peaks in I_{65} lead to relative minima in V and a subsequent decrease in both A and F, which may induce negative F values that trigger the oceanic CO_2 emission. The condition to generate a deglaciation is, thus, the occurrence of a maximum of I_{65} in a period

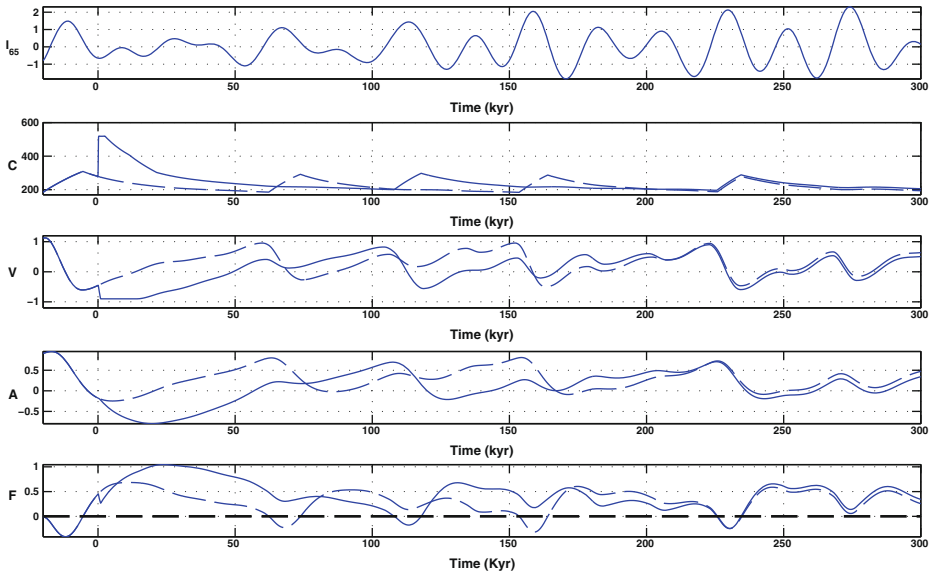

Fig. 7 Prediction of climatic variables for the future 300 kyr as obtained using the 3τ model (including weathering compensation and methane emissions). The *top panel* shows the I_{65} insolation time series and all other four panels present the projection of (*second panel*) dimensional atmospheric CO_2 concentrations, (*third panel*) normalized ice volume, (*fourth panel*) normalized extension of Antarctic ice sheet, and (*bottom panel*) stratification function, with (*solid line*) and without (*dashed line*) the anthropogenic perturbation

when V is large. This double condition was observed and incorporated by Paillard in some previous models (Paillard 1998).

The model predicts a maximum CO_2 concentration of 519 ppmv in 2300 AD followed by an exponential decay. To define interglacial conditions we use two simple criteria (Crucifix 2011): CO_2 concentrations above 250 ppm and benthic $\delta^{18}O$ below 3.8 per mil; the CO_2 criterion has been used also by IPCC (2007). According to the CO_2 criterion the current interglacial would end 40 kyr AP (35 kyr AP) for 3τ (LS), and according to the $\delta^{18}O$ criterion it would end 46 kyr AP (40 kyr AP) for 3τ (LS). Therefore, the length of this interglacial would be 54–47 kyr (according to the CO_2 values) and 58 - 50 kyr (according to the $\delta^{18}O$) as predicted by the 3τ and LS models. This interglacial would be followed by a glacial period lasting until 113 kyr AP.

The model also predicts the disappearance of the next interglacial unperturbed age, which should start at 64 kyr AP. This is due to the abnormally reduced ice volume and ice sheet area predicted for the present interglacial, which takes long to recover. The ice sheet, A, follows the evolution of V with a delay of about 7 kyr (Eq. 2a and τ_A value in Table 1). The F function, however, turns negative only when A is large enough (due to the high value $b = 1.205$). At 64 kyr AP, V decreases (C rises) in response to the positive forcing of the I_{65} insolation but A is not high enough for F to become negative. If V and A were large, as occurs in the unperturbed case, F would be close to the threshold value ($F = 0$) and the decrease of V (rise of C) at that time would drive F to negative values, triggering the oceanic pulse. This delayed recovery of the ice volume V (and A) is caused by the anthropogenic pulse introduced in the model, which produces 20 kyr of abnormally high greenhouse effect. Under these conditions V needs more time to reach the glacial maximum and the next glacial cycle moves 44 kyr forward in time. At 235 kyr AP perturbed and

unpertubed interglacials coincide again and the further evolution of all variables remains in phase, suggesting the recovery of the natural periodicity.

We have also explored how sensitive are the model results, in particular the starting time for the next interglacial cycle, to different URR values. One main result is that a progressive increase in the anthropogenic pulse leads to smaller, with lower CO_2 values, interglacial cycles. A quite relevant result is that the timing for the next interglacial will change discretely as U exceeds different threshold values (inset in Fig. 6). For example $U = 475$ Gt represents the URR threshold beyond which the next interglacial will experience a delay of 44 kyr; the following thresholds will occur at 1725 and 2100 Gt, with corresponding additional delays of 42 and 72 kyr (inset in Fig. 6).

5 Discussion

Let us consider first the projections for an unperturbed present interglacial. It may be argued that the carbon mechanisms in our models are too simplistic to represent adequately the interglacial of 400 kyr BP, which is the closest natural analogue of the present interglacial (Loutre and Berger 2000). This is partially true, since the CO_2 plateau near 400 kyr BP is not reproduced by our models, which always produce saw-teeth shapes for the CO_2 evolution. However, if we apply the Crucifix (2011) CO_2 and $\delta^{18}O$ criteria, the models do reasonably well. According to $\delta^{18}O$, the duration of the 400 kyr BP interglacial is 26 kyr from the proxies, 21 kyr from model LS and 27 kyr from model 3τ; the corresponding CO_2 durations are 44 kyr (proxy), 27 kyr (LS) and 35 kyr (3τ). In addition, Fig. 1 (panel 2) shows that near 400 kyr BP the shape of the glacial termination and the beginning of the interglacial are well simulated by both LS and 3τ. This endorses the potential of our models (particularly, model 3τ) to correctly anticipate the duration of the present unperturbed interglacial.

Loutre and Berger (2000) predict that the unperturbed present interglacial is destined to last about 55 kyr if the CO_2 concentrations are maintained at constant levels above 220 ppmv. That long interglacial duration is supposedly due to the configuration of the astronomic forcing, which is similar to the one occurred in the interglacial of 400 kyr BP. With a CO_2 level of 210 ppmv they foresee an interglacial lasting until 15 kyr AP; with 220 ppmv they predicted the glacial conditions would start 17 kyr AP and the interglacial conditions would return between 27 and 54 kyr AP. The comparison with our results is difficult, because our models depend on three characteristic times of CO_2 absorption after the interglacial peak, making CO_2 not to remain constant in time. If we use the $\delta^{18}O$ criterion, the end of the present unperturbed interglacial is estimated at 12.5 kyr AP; the estimate becomes 8 kyr AP if the CO_2 criterion is used (for both 3τ and LS models). Thus, the duration of the unperturbed interglacial as predicted by our models (20 kyr - 25 kyr for $CO_2 - \delta^{18}O$) is less than Loutre and Berger (2000) estimate for CO_2 concentrations above 220 ppmv, but similar to their prediction with CO_2 concentration of 210 ppmv.

After adding the anthropogenic perturbation, the 3τ model predicts a slow decay of the greenhouse effect so that the interglacial conditions remain until 40–46 kyr AP, which is shorter than predicted by Loutre and Berger (2000) (55 kyr) for their high-CO_2 concentration ($\geq$210 ppmv) scenario, and longer than the duration of previous interglacials (30 kyr or less according to Winograd et al. (1997)).

Our prediction for the following perturbed interglacial is not strongly dependent on the exact value of the CO_2 initial condition in the URR range of 475–1700 Gt (inset in Fig. 6). When URR is equal or larger than 1725 Gt, the models predict a very slow V, A and F

recovery, so that the interglacial at 118 kyr AP is lost and the next interglacial takes place in coincidence with the following obliquity maximum at 160 kyr AP. For URR between 2100 and 2500 Gt, the recovery is even slower, shifting the next interglacial to 232 kyr AP, and for URR equal or larger than 2525 Gt the next interglacial is totally lost until at least 300 kyr AP. This would be the case with the most extreme IPCC scenarios (such as A1F1 and A1G AIM); however, we consider those scenarios with URR above 2100 Gt as unrealistic.

Our projection also displays some interesting resemblances with Mysak (2008) forecast, carried out with the McGill Paleoclimate Model, an Earth System Model of Intermediate Complexity. If we set the interglacial conditions to correspond to CO_2 concentrations above 250 ppmv (IPCC 2007), our 3τ model does show a perturbed interglacial lasting until 46 kyr AP. This is close to Mysak's prediction (2008), who found that the next glacial inception occurs 50 kyr AP.

On the other hand, our prediction differs substantially from the results of the intermediate complexity model by Archer and Ganopolski (2005). Their carbon model, based on Archer (2005), includes very plausible geochemical mechanisms for ocean acidification and $CaCO_3$ response operating at the scales of 10 kyr and 100 kyr. However, their evolution of atmospheric pCO_2 does not account for the sort of natural pCO_2 variability that drives the glacial/interglacial cycles, and only focuses on the geochemical mechanisms that credibly affect the anthropogenic perturbation. The lack of mechanisms for the geophysical absorption of CO_2 at time scales of 10 kyr, such as the ice volume - CO_2 feedback, probably results in predictions for the atmospheric pCO_2 that are substantially higher than ours. For a total carbon emission of 1000 Gt, their model forecasts the current interglacial period to last for another 130 kyr. In contrast, we project a much smaller effect of the anthropogenic pulse, with the atmospheric CO_2 decreasing below interglacial levels in 40-46 kyr (according to 3τ) and reaching the minimum glacial levels in about 100 kyr, resulting in a delay of the next interglacial stage by 44 kyr.

The differences between the results of Archer and Ganopolski (2005) and Mysak (2008) arise from the different hypotheses on the long-term fate of atmospheric CO_2, which is made to depend exclusively on geochemical mechanisms in the former, and is externally imposed in the latter. In comparison, in our models the rate of decay for most of the atmospheric CO_2, except for the relatively small anthropogenic fraction (9 %) which is assumed to obey a long-term weathering adjustment, is obtained through fitting the model equations to the observed CO_2 and global ice volume variations during the past glacial cycles. The time decay constants obtained in this way lie between 8400 and 13500 yr (Table 1). Our underlying assumption, therefore, is that the internal dynamics of the Earth system will remain the same, either with or without the anthropogenic CO_2 pulse, except for the relatively small fraction with a weathering-related slow decay.

6 Summary and conclusions

In this work we have illustrated an application of two simple relaxation-type models (García-Olivares and Herrero 2012b) to predict the future evolution of global Earth variables during the next 300 kyr, with and without the atmospheric CO_2 perturbation caused by anthropogenic fossil fuels emissions.

The abnormally high thermal perturbation of the current interglacial will lead to a delay in the future advance of the ice sheet over the Antarctic shelf. As a result, the relative maximum of boreal insolation 65 kyr AP will have no effect on the stability of the developing

glaciation. However, the following insolation peak (115 kyr AP) will take place in an appropriate state of the climate system and will be sufficient to induce the new deglaciation. The next glacial maximum will take place about 105 kyr AP and the following interglacial will be delayed forward in time by 44 kyr in relation to unperturbed conditions. Our models projections depend on the URR value, being very stable in the 475 to 1700 Gt range; for URR equal or larger than 1725/2100 Gt the next interglacial is expected to begin 160/232 kyr AP.

Our projection on the evolution of the Earth's climate may be compared with those from intermediate complexity models for the Earth System, with appealing similarities in one case (Mysak 2008) but with differences in another instance (Archer and Ganopolski 2005). We believe that simple coupled models have the fundamental attribute that, despite their simple structure, retain the principal Earth's climatic interactions, being capable of accounting for the natural evolution of an externally imposed atmospheric CO_2 pulse. Nevertheless, in order to confirm this claim, our results should be compared with those obtained from an Earth system model which includes fully interactive long-term global carbon dynamics. Once this is proven, simple coupled models may become a helpful tool to examine the future evolution of climate under different scenarios of anthropogenic fossil fuels emissions.

Acknowledgments This study has been carried out in the framework of project TIC-MOC (CTM2011-28867), funded by the 2008-2011 Spanish R+D Plan. C. Herrero acknowledges a CSIC JAE-Predoc scholarship co-financed by the European Social Fund (FSE). We thank Carles Pelejero and Eva Calvo for their help with proxy data and their useful support and also to Didier Paillard for his interesting suggestions. Some useful discussions were held with Anna Cabré, Xiaorong Li and Levin Nickelsen, participants of a supervised work carried out as part of the Ramon Margalef Summer Colloquium held in Barcelona between 1 and 13 July 2013. The authors would also like to sincerely thank three anonymous reviewers whom greatly helped to improve the manuscript.

References

Archer D (2005) Fate of fossil fuel CO_2 in geologic time. J Geophys Res 110:C09S05

Archer D, Ganopolski A (2005) A movable trigger: fossil fuel co2 and the onset of the next glaciation. Geochem Geophys Geosyst 6(5):Q05,003. doi:10.1029/2004GC000891

Archer D, Winguth A, Lea D, Mahowald N (2000) What caused the glacial/interglacial atmospheric pCO_2 cycles? Rev Geophys 38(2):159–189. doi:10.1029/1999RG000066

Archer D, Buffett B, Brovkin V (2009) Ocean methane hydrates as a slow tipping point in the global carbon cycle. Proc Natl Acad Sci 106(49):20,596–20,601. doi:10.1073/pnas.0800885105. http://www.pnas.org/content/106/49/20596.abstract, http://www.pnas.org/content/106/49/20596.full.pdf+html

Berg P, Boland A (2013) Analysis of ultimate fossil fuel reserves and associated co2 emissions in ipcc scenarios. Nat Resour Res. doi:10.1007/s11053-013-9207-7

Berger A (1978) Long term variations of daily insolation and quaternary climatic changes. J Atmos Sci 35(12):2362–2367

Bintanja R, van de Wal RS, Oerlemans J (2005) Modelled atmospheric temperatures and global sea levels over the past million years. Nature 437:125–128

Boden A, Marland G, Andres R (2010) Global, regional, and national fossil-fuel CO_2 emissions. Tech. rep., Carbon dioxide information analysis center, Oak Ridge National Laboratory, U.S. Department of Energy

Crucifix M (2011) How can a glacial inception be predicted? The Holocene 21(5):831–842. doi:10.1177/0959683610394883. http://hol.sagepub.com/content/21/5/831.abstract, http://hol.sagepub.com/content/21/5/831.full.pdf+html

Energy Watch Group (2007) Coal: resources and future production. EWG-Series No 1/2007 1

García-Olivares A, Herrero C (2012a) Fitting the last pleistocene delta o-18 and CO_2 time-series with simple box models. Sci Mar 76S1:209–218. http://www.icm.csic.es/scimar/index.php/secId/7/IdArt/4128/

García-Olivares A, Herrero C (2012b) Simulation of glacial-interglacial cycles by simple relaxation models: consistency with observational results. Clim Dyn 41(5–6):1307–1331. doi:10.1007/s00382-012-1614-7

Gassan-zade O (2004) National ghg emission factors in former soviet union countries. TSU Internship Report, IPCC NGGIP/IGES p 53

Grinsted A, Moore J, Jevrejeva S (2004) Application of the cross wavelet transform and wavelet coherence to geophysical time series. Nonlin Processes Geophys 11:561–566

Hays JD, Imbrie J, Shackleton NJ (1976) Variations in the earth's orbit: pacemaker of the ice ages. Science 194(4270):1121–1132. http://www.sciencemag.org/content/194/4270/1121.abstract, http://www.sciencemag.org/content/194/4270/1121.full.pdf

Höök M, Sivertsson A, Aleklett K (2010) Validity of the fossil fuel production outlooks in the IPCC emission scenarios. Nat Resour Res 19:63–81. doi:10.1007/s11053-010-9113-1

IEA (2010) World energy outlook. Tech. rep., International Energy Agency. http://www.worldenergyoutlook.org/publications/weo-2010/

IEA (2012) World energy outlook. Tech. rep., International Energy Agency. http://www.worldenergyoutlook.org/publications/weo-2012/

Indermuhle A, Monnin E, Stauffer B, Stocker TF, Wahlen M (2000) Atmospheric CO_2 concentration from 60 to 20 kyr BP from the Taylor Dome Ice Core, Antarctica. Geophys Res Lett 27(5):735–738. doi:10.1029/1999GL010960

IPCC (2001) Climate change 2001: the scientific basis. Contribution of working group I to the 3rd assessment report of the intergovernmental panel on climate change. Cambridge University Press, Cambridge

IPCC (2007) Contribution of working group I to the 4th assessment report of the intergovernmental panel on climate change, vol 6. Paleoclimate, Fig. 6.3. Cambridge University Press, Cambridge. http://www.ipcc.ch/publications_and_data/ar4/wg1/en/contents.html

Jain A, Kheshgi H, Wuebbles D (1994) Integrated science model for assessment of climate change model. In: Proceedings of air and waste management association 87th annual meeting, Cincinnati

Kheshgi HS, Jain AK (2003) Projecting future climate change: implications of carbon cycle model intercomparisons. Glob Biogeochem Cycles 17(2). doi:10.1029/2001GB001842

Laherrere J (2006) Fossil fuels: what future? In: Proceedings of the Workshop on Global Dialogue on Energy Security. The Dialogue International Policy Institute, China Institute of International Studies, Beijing

Laherrere J (2012a) ASPO: lessons learned: successes and challenges. In: 10 years of ASPO: lessons learned. http://www.aspo2012.at/wp-content/uploads/2012/06/Laherrere_ASPOViennaJL28may.pdf

Laherrere J (2012b) Update on coal. The oil drum. http://www.theoildrum.com/node/9583

Lisiecki LE, Raymo ME (2005) A Pliocene-Pleistocene stack of 57 globally distributed benthic delta O-18 records. Paleoceanography 20(1):PA1003. doi:10.1029/2004PA001071

Loutre M, Berger A (2000) Future climatic changes: are we entering an exceptionally long interglacial? Clim Chang 46:61–90. doi:10.1023/A:1005559827189

Luthi D, Le Floch M, Bereiter B, Blunier T, Barnola JM, Siegenthaler U, Raynaud D, Jouzel J, Fischer H, Kawamura K, Stocker TF (2008) High-resolution carbon dioxide concentration record 650,000–800,000 years before present. Nature 453(7193):379–382. doi:10.1038/nature06949

Marwan N, Kurths J (2002) Nonlinear analysis of bivariate data with cross recurrence plots. Phys Lett A 302(5–6):299–307

Marwan N, Romano MC, Thiel M, Kurths J (2007) Recurrence plots for the analysis of complex systems. Phys Rep 438(5–6):237–329

Monnin E, Indermuhle A, Dallenbach A, Fluckiger J, Bernhard S, Stocker TF, Raynaud D, Barnola JM (2001) Atmospheric CO_2 concentrations over the last glacial termination. Science 291:112–114

Mysak LA (2008) Glacial inceptions: past and future. Atmosphere-Ocean 46(3):317–341. doi:10.3137/ao.460303. http://www.tandfonline.com/doi/abs/10.3137/ao.460303, http://www.tandfonline.com/doi/pdf/10.3137/ao.460303

Paillard D (1998) The timing of pleistocene glaciations from a simple multiple-state climate model. Nature 391(6665):378–381. doi:10.1038/34891

Paillard D (2006) What drives the ice age cycle? Science 313(5786):455–456. doi:10.1126/science.1131297. http://www.sciencemag.org/content/313/5786/455.short, http://www.sciencemag.org/content/313/5786/455.full.pdf

Paillard D (2010) Climate and the orbital parameters of the Earth. Compt Rendus Geosci 342(4–5):273–285. http://www.sciencedirect.com/science/article/pii/S1631071310000052

Paillard D, Parrenin F (2004) The Antarctic ice sheet and the triggering of deglaciations. Earth Planet Sci Lett 227(3–4):263–271. http://www.sciencedirect.com/science/article/pii/S0012821X04005564

Petit JR, Jouzel J, Raynaud D, Barkov NI, Barnola JM, Basile I, Bender M, Chappellaz J, Davis M, Delaygue G, Delmotte M, Kotlyakov VM, Legrand M, Lipenkov VY, Lorius C, Pepin L, Ritz C, Saltzman E, Stievenard M (1999) Climate and atmospheric history of the past 420000 years from the Vostok ice core Antarctica. Nature 399:429–436

Siegenthaler U, Stocker TF, Monnin E, Luthi D, Schwander J, Stauffer B, Raynaud D, Barnola JM, Fischer H, Masson-Delmotte V, Jouzel J (2005) Stable carbon cycle-climate relationship during the late pleistocene. Science 310:1313–1317

Sigman DM, Boyle EA (2000) Glacial/interglacial variations in atmospheric carbon dioxide. Nature 407(6806):859–869. doi:10.1038/35038000

SRES (2000) Special report on emissions scenarios, report prepared by the intergovernmental panel on climate change (IPCC) for the 3rd assessment report. Tech. rep., UN

Winograd IJ, Landwehr JM, Ludwig KR, Coplen TB, Riggs AC (1997) Duration and structure of the past four interglacials. Quatern Res 48:141–154